SUPPLEMENTAL MATERIAL

miR-146a Suppresses SUMO1 Expression and Induces Cardiac Dysfunction in Maladaptive Hypertrophy

Jae Gyun Oh[1],Shin Watanabe[1], Ahyoung Lee[1], Przemek A. Gorski[1], Philyoung Lee[1], Dongtak Jeong[1], Lifan Liang[1], Yaxuan Liang[1], Alessia Baccarini[2], Susmita Sahoo[1], Brian D Brown[2], Roger J. Hajjar[1]* and Changwon Kho[1]*

Short title: miR-146a Suppresses SUMO1 Expression

EXPENDED METHODS

All data have been made publicly available at figshare and can be accessed at 10.6084/m9.figshare.6932888 or from the corresponding author on request.

Luciferase Reporter Assay.

The entire human SUMO1-3' UTR segment (nm_001005781), which was subcloned into pMirTarget vector (OriGene), was transfected into H9C2 cell line with human miR-146a mimic (Exiqon) or control miR mimic (cel-mir-67, Dharmacon) using a Viromoer (Lipocalyx) transfection reagent. After 48 hrs, cells were assayed using a luciferase assay kit (Promega). The putative binding site in SUMO1-3' UTR was point-mutated from AAGUUCU to A**C**G**GG**C**G** to blunt its binding capacity by PCR-based mutagenesis. Plasmid DNA was sequenced to ensure its authenticity. The primer pairs used were as follows: GTC AGA AGA TCC CAG AAA CGG GCG AAT TTT CAT TAG CAA TTA ATA AAGC (forward), GCT TTA TTA ATT GCT AAT GAA AAT TCG CCC GTT TCT GGG ATC TTC TGAC (Reverse).

miR Target Search.

To identify specific miRs which target SUMO1, four sequence-based prediction programs (microRNA.org, miRserch, DIANA, mirdb.org) were used. By overlapping the lists of candidate sequences from the prediction programs, miR-146a was selected as the most probable miR which targets the SUMO1 gene.

Fluorescence-activated Cell Sorting (FACS) Analysis.

Non-myocyte fraction from Langendorff-based isolation was stained on ice in PBS containing 6% FCS and 4 mmol/L EDTA using the following antibodies: CD31 (FITC, Bio legend, Cat# 102406, 1:200), CD45 (APC/cy7, BD Biosciences, Cat# 557659, 1:100) or isotype controls IgG2a (BD Biosciences, Cat# 553454). Positive sorting gates for the CD31 positive or CD45 were set according to unstained controls, isotype controls and single staining controls. Cell sorting was performed on a BD FACS Aria III (BD Biosciences) with 100 μm nozzle. The endothelial cells were defined by the markers $CD31^+$ and $CD45^-$; leukocytes by $CD31^-$ and $CD45^+$; and fibroblasts by $CD31^-$ and $CD45^-$. For fibroblast purity analysis, FACS isolated cells were fixed with 2% PFA, permeabilized and stained in α-SMA (Abcam) or FAP (Abcam) with Vimentin (Abcam). The RNA was extracted from the sorted cells and analyzed.

Cell Culture and EV Purification.

Cardiac fibroblasts were isolated from mouse hearts by FACS as described above. Cells were resuspended in fresh medium containing 10% FBS and plated on 60 mm^2 culture plates at 37 °C with 5% CO_2 for 48 hrs. The culture medium was then changed to medium containing 1% EV-depleted FBS (FBS was

depleted of contaminating bovine EVs by ultracentrifugation for 6 h at 100,000 g) or 10% EV-depleted FBS and TGF-β (10 ng/mL). These cells were labeled as Fib or Fib + TGF-β, respectively. Cultured media was collected after 48 hrs, and EVs purified by several centrifugations according to a previously described protocol.[27] EVs were pelleted by ultracentrifugation at 100,000 × g at 4 °C for 90 min and resuspended in 200 μL of PBS solution. To generate miR-146a-enriched or depleted EVs, cultured fibroblasts were infected with Ad_pre-mir-146a or Ad_decoy-146a for 48hrs and EVs in the cultured medium were isolated. To evaluate miR-146a secretion, macrophages (Cell biologics) were cultured in RPMI-1640 medium (Sigma) containing 10% EV-depleted FBS and analyzed as described above.

Cardiac EV Purification.

To analyze cardiac EVs from the heart tissue, Langendorff-based isolation was applied. Following the digestion of connective tissues as described above, the cardiac cells were separated by low-speed centrifugation and further analyzed with FACS. The cardiac EVs were purified by differential centrifugation from the remaining supernatant, and the particle numbers were counted by the nanoparticle tracking analysis (NTA).

Cardiomyocyte Isolation.

All animals were housed and treated in accordance with guidelines from the NIH and institutional animal care and use committees (IACUC), and the protocols used were approved by the Mount Sinai School of Medicine animal care and use committee. Cardiomyocytes were isolated from B6C3/F1 mouse hearts by the Langendorff-based method as previously described[1, 2] with minor modifications. Male mice of 6-8 weeks of age (25-30 g) were used. In brief, after a quick removal of the heart from the chest, the aorta was retrogradely perfused at 37 °C for 3 min with calcium-free Tyrode buffer (137 mmol/L NaCl, 5.4 mmol/L KCl, 1 mmol/L $MgCl_2$, 10 mmol/L glucose, 10 mmol/L HEPES [pH 7.4], 10 mmol/L 2, 3-butanedione monoxime, and 5 mmol/L taurine) gassed with 100% O_2. The enzymatic digestion was initiated by the addition of collagenase type B (300 U/mL; Worthington) and hyaluronidase (0.1 mg/mL; Worthington) to the perfusion solution. When the heart became swollen after 20 min of digestion, the left ventricle was quickly removed, cut into several chunks, and gently pipetted for 2 minutes in calcium-free Tyrode buffer with 5% BSA. The supernatant containing the dispersed myocytes was filtered through a cell strainer (100 μm pore size; BD Falcon) and gently centrifuged at 50 g for 1 min. Most myocytes settled to a pellet, while crude non-myocyte fraction remained in suspension. The non-myocyte fraction was further sorted and analyzed by FACS analysis. This procedure usually yielded ≥ 80% viable rod-shaped ventricular myocytes with clear sarcomere striations. Myocytes with obvious sarcolemmal blebs or spontaneous contractions were not used.

Adenoviruses.

Adenoviruses encoding pre-mir-146a and decoy-146a were generated using the pAdEasy XL adenoviral vector system (Stratagene) according to the manufacturer's protocols. Briefly, the entire human pre-mir-146a (MI0000477; OriGene) and decoy-146a segment were subcloned into the NotI/SalI site of pShuttle-IRES-hrGFP vector (Stratagene). The decoy-146a sequence was kindly donated by Dr. Brian D. Brown (Icahn School of medicine at Mount Sinai). The isolated cardiomyocytes were infected with Ad_β-gal, Ad_pre-mir-146a or Ad_decoy-146a at an indicated MOI for 24 or 48 hrs.

Adeno-associated Viruses.

Self-complementary AAV (serotype 9) constructs were generated using the pds-AAV2-EGFP vector. The human pre-mir-146a and decoy-146a segment were subcloned into the MluI/HpaI site of pdsAAV2-EGFP. The recombinant AAV was produced by transfecting 293T cells as previously described.[3] The AAV particles in the cell culture media were precipitated with ammonium sulfate and purified by ultracentrifugation on an iodixanol gradient. The particles were then concentrated using a centrifugal concentrator. The AAV titer was determined by qRT-PCR and SDS-PAGE. rAAV9_LacZ, rAAV9_pre-mir-146a or rAAV9_decoy-146a (5×10^{11} viral genome/mouse) was injected into the tail vein of B6C3/F1 mice, and the phenotype of the heart was examined after 4 weeks.

Quantitative Real-time (qRT)-PCR.

Total RNA was isolated with mirVana miRNA isolation kit (Ambion). Reverse transcription was performed using qScript microRNA cDNA Synthesis Kit (Quanta). PCR was performed using an ABI PRISM Sequence Detector System 7500 (Applied Biosystems) with SYBR Green (Quanta) as the fluorescent dye and ROX (Quanta) as the passive reference dye. The cycle number at which the reaction crossed an arbitrarily-placed threshold (C_T) was determined for each gene and the relative amount of each gene to 18S rRNA was used to quantify cellular RNA. Briefly, the average of the Ct values for the loading control gene (in our case, 18S) and the gene tested (miR-146a) in the experimental (HF) and control conditions (NF) were measured by qRT-PCR. Then, the differences between HF, miR-146a and HF, 18S ($Ct^{TAC,miR\text{-}146a} - Ct^{TAC,18S}$) and NF, miR-146a and NF, 18S ($Ct^{NF,miR\text{-}146a}$-$Ct^{NF,18S}$) were calculated (ΔCt^{HF}, ΔCt^{NF}, respectively).

$\Delta Ct^{HF} = Ct^{TAC,miR\text{-}146a} - Ct^{TAC,18S}$, $\Delta Ct^{HF} = Ct^{NF,miR\text{-}146a}$-$Ct^{NF,18S}$

Then, once again the difference between ΔCt^{HF} and ΔCt^{NF} (ΔCt^{HF}-ΔCt^{NF}), the Double Delta Ct Value, was calculated. Finally, the fold change is calculated based on the formula shown below:

Fold change = $2^{-\Delta\Delta Ct} = 2^{-(\Delta CtHF - \Delta CtNF)}$

Due to the absence of well-characterized internal controls for microRNAs in cardiac EVs, absolute quantification was used to validate the EV miR-146a copy number. A standard curve was calculated using the linear range of the dilution series (5×10^1-5×10^{11} copy number/μL) and used for absolute quantification of the miR-146a in EV RNA. For the cellular RNA quantification, the primers used for qRT-PCR were as follows:
miR-146a, 5'-TGA GAA CTG AAT TCC ATG GGTT-3' miR-146b, 5'-TGA GAA CTG AAT TCC ATA GGC TG-3' and PerfeCTa universal reverse primer (Quanta); pri-mir-146a, 5'-TGA GAA CTG AAT TCC ATG GGTT-3' and 5'-ATC TAC TCT CTC CAG GTC CTCA -3'; mouse SUMO1,5'-TAG CAG TGA GAT ACA TTT CAA AGTG-3' and 5'-GAC CTT CAA AGA GAA ACC TGA GTG-3'; mouse SERCA2a, 5'-GCT GAA GCG ACC CAC ACT-3' and 5'-ACA GCT GTC CCC TCC TTT TT-3'; IRAK1, 5'-GGG CGG TGA TGA GGA ACA-3' and 5'-CCA CTC CAG GTC AGC GTT CT-3'; TRAF6, 5'-CCA TGC GGC CAT AGG TTCT-3' and 5'-TTG TGA CCT GCA TCC CTT ATTG-3'; 18s, 5'-TAA CGA ACG AGA CTC TGG CAT-3' and 5'-CGG ACA TCT AAG GGC ATC ACAG-3'.

Western Blot and SUMOylation Analysis.

Western blotting and SUMOylation assay were conducted as previously described with minor modifications.[1] Briefly, isolated cardiomyocytes were infected with adenovirus encoding pre-mir-146a or decoy-146a at an MOI of 50 for 24 hrs. The cells were lysed in ice-cold lysis buffer (50 mmol/L Tris-HCl [pH 8.0], 150 mmol/L NaCl, 0.1% Triton X-100, 10 mmol/L EDTA, complete protease inhibitor (Roche), and 20 mmol/L N-ethylmaleimide). For Western blot analysis, approximately 50 μg of protein from each sample was separated by SDS-PAGE and transferred to PVDF membranes (Schleicher & Schuell). The membranes were blocked with 5% non-fat milk and then incubated with primary antibodies at 4°C overnight. The membranes were incubated with secondary antibodies conjugated to horseradish peroxidase (Jackson ImmunoResearch) and then developed with a chemiluminescent substrate (Perkin Elmer). For SUMOylation assay, cell lysates were immunoprecipitated overnight at 4 °C with SUMO1 antibody-conjugated beads (Santa Cruz Biotech, sc-5308ac). After washing in cold lysis buffer, the immunocomplexes were immunoblotted with a SERCA2a-specific antibody. For SUMOylation assay with tissue extracts, hearts from each experimental and control group were frozen in liquid nitrogen. The frozen tissues were crushed and homogenized in lysis buffer using the MP homogenization system (FastPrep homogenizer). Tissue lysates were immunoprecipitated and immunoblotted as described above. The antibodies used were as follows: SUMO1 (R&D Systems, AF3289, 1:1000); SERCA2a (custom antibody from 21st Century Biochemicals, 1:3000); GAPDH (Sigma, G8795, 1:10000).

Ca^{2+} Transient and Contractility Measurement.

The mechanical properties of ventricular myocytes were assessed through the use of a video-based edge detection system (IonOptix) as previously described.[1, 2] In brief, a laminin-coated coverslip with cells attached was placed in a chamber mounted on the stage of an inverted microscope (Motic AE31) and was perfused (about 1 mL/min at 37 °C) with Tyrode buffer. Cardiomyocytes were stimulated to contract at 0.5 Hz. Changes in sarcomere length during shortening and relengthening were captured and analyzed using soft edge software (IonOptix). The cardiomyocytes were loaded with 0.5 μmol/L Fura2-AM (Life technology), a Ca^{2+}-sensitive indicator, for 10 min at 37 °C. Fluorescence emissions were recorded by IonOptix simultaneously with contractility measurements.

Transverse Aortic Constriction.

TAC surgery was performed as previously described.[3] Briefly, 6-8 week old male mice (25-30 g) were anesthetized by ketamine/xylazine cocktail (5:1 ratio). The A longitudinal incision of 2 to 3 mm was made in the proximal sternum to allow visualization of the aortic arch, and the transverse aorta was ligated between the innominate and left common carotid arteries with an overlaid 27-gauge needle. The needle was then immediately removed, leaving a discrete region of constriction. To evaluate the consistency of the TAC model, pressure gradients, fractional shortening and wall thickness were tested by echocardiography. Then, the qualified animals were randomly allocated into two groups by a randomizing software (www.randomizer.org). A <5% difference in the mean of fractional shortening (FS), interventricular septum thickness at end-diastole (IVSd), and body weight were present among the experimental groups (Table XI). Sham-operated animals underwent the same surgical procedures, except that the ligature was not tied.

Echocardiography.

Transthoracic echocardiography was performed using a Vivid 7000 (GE Healthcare) equipped with a H13L transducer (14 MHz). Two-dimensional and M-mode images were obtained in the short-axis view. The heart rate, left ventricular end-diastolic internal diameter and left ventricular end-systolic internal diameter were measured in at least three repeated cardiac cycles. The ejection fraction and fractional shortening were then calculated.

Hemodynamics.

Hemodynamic measurements were performed using a 1.2 Fr pressure-volume conductance catheter (Scisense). Pressure-volume loop analysis was performed as previously described.[3] Mice were injected intraperitoneally with urethane (1 g/kg), etomidate (10 mg/kg) and morphine (1 mg/kg) and mechanically ventilated with 7 μL/g stroke volume at 125 respirations/min. The chest was opened to expose the heart

for an apical stab approach. To determine absolute ventricular volumes via admittance technology, myocardial and blood conductance were obtained before pressure-volume catheter placement in the left ventricle. The inferior vena cava was transiently occluded to reduce ventricular pre-load to obtain load-independent pressure-volume relationships. Hemodynamic measurements were acquired and analyzed using IOX software (EMKAtech).

Immunohistochemistry.

The hearts from the mice subjected to TAC surgery and then injected with control virus or rAAV9_decoy-146a were frozen in optimal cutting temperature compound (Sakura Finetek), sectioned, and stained with primary rabbit CD45 (Abcam, ab10558) or TNFα (Abcam, ab6671) antibody at 1/150 dilution overnight at 4°C. Sections were conjugated with HRP antibody (Vector Laboratories) at room temperature for 2 h then covered with DAB (Vector Laboratories), nuclei were counterstained in hematoxylin, and slides were mounted with Vectashield mounting medium (Vector Laboratories). Subsequently, all fields were observed under light microscopy (Nikon) at ×10 magnification. Control experiments without primary antibody demonstrated that the signals observed were specific. Positive areas for CD45 and TNFα were semi-quantified by an image processing program (ImageJ) and represented as the percentage of total heart area.

Nanoparticle Tracking Analysis (NTA).

Samples were loaded into the assembled sample chamber of a NanoSight LM10. 60-second video images were acquired by a Hamamatsu C11440 ORCA-Flash 2.8 digital camera and analyzed by NanoSight NTA 2.3 software.

SUPPLEMENTAL FIGURES AND FIGURE LEGENDS

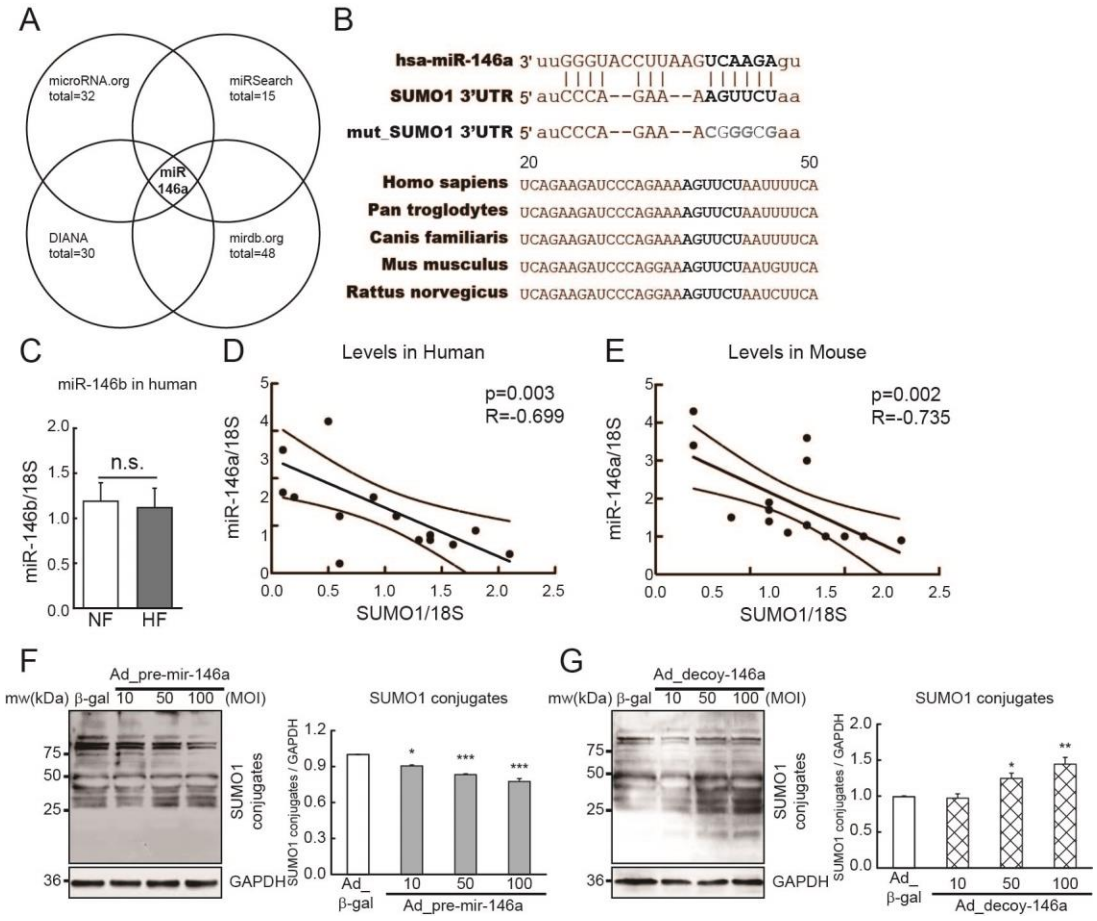

Figure I. SUMO1 mRNA is a specific target of miR-146a in cardiomyocytes.

A, Schematic diagram for *in silico* prediction of SUMO1-targeting microRNAs. **B,** Sequence alignment and evolutionary conservation between miR-146a and its putative binding sites in the 3′UTR of SUMO1 mRNA from several indicated species (sequences recognized by miR-146a seed sequence is shown in bold). UTR, untranslated regions; mut, point mutated; Homo sapiens, human; Pan troglodytes, chimpanzee; Canis Familiaris, dog; Mus musculus, mouse; Rattus norvegicus, rat. **C,** Changes in SUMO1 mRNA and miR-146a levels in human hearts of non-failing (NF) and heart failure (HF) patients (n=7-9). **D,** Changes in SUMO1 mRNA and miR-146a levels in mouse hearts of sham and TAC-operated mice (6 weeks after TAC) (n=8-9). **E,** Changes in miR-146b levels in human hearts of non-failing (NF) and heart failure (HF) patients (n=7-9). R: Spearman correlation coefficient **F** and **G,** The patterns of global SUMOylation in isolated adult mouse cardiomyocytes which were infected with an adenovirus encoding pre-mir-146a (Ad_pre-mir-146a) (**F**) or miR-146a decoy (Ad_decoy-146a) (**G**) for 48h. n=3, **, p<0.01,

***, p<0.001 versus the respective control, as determined by Student's *t*-test. Data are presented as mean ± s.e.m.

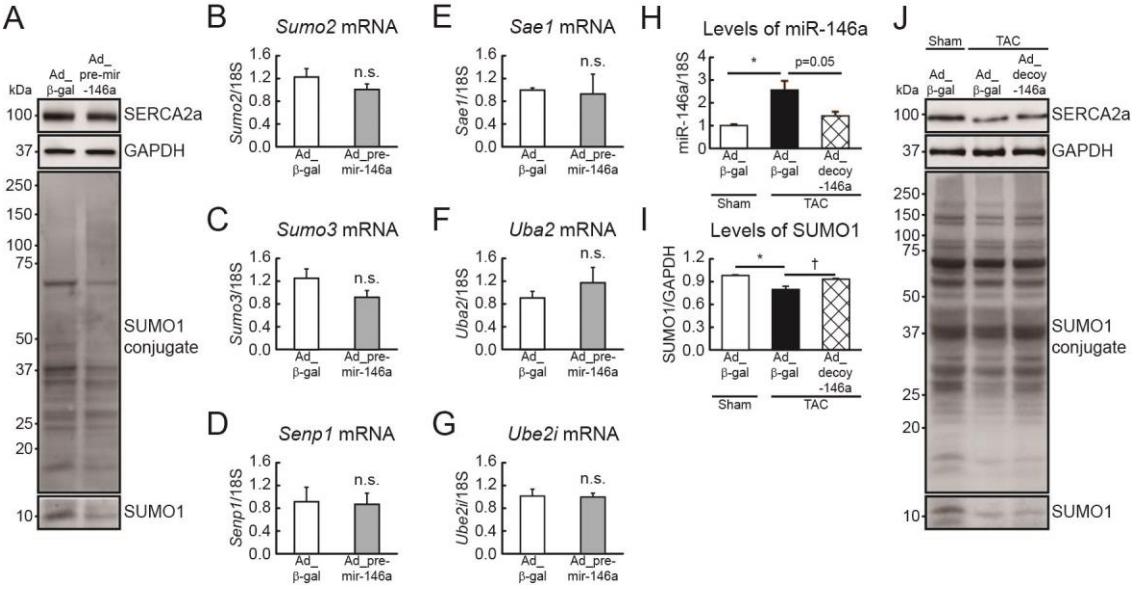

Figure II. miR-146a does not affect the expression of other SUMOylation enzymes.

A, Representative blot showing SERCA2a, SUMO1 and total SUMO1 conjugates after infection of isolated cardiomyocytes with Ad_pre-mir-146a. **B-G,** mRNA quantification of *Sumo2* (**B**), *Sumo3* (**C**), *Senp1* (**D**), *Sae1* (**E**), *Uba2* (**F**) and *Ube2i* (**G**) in isolated adult cardiomyocytes infected with Ad_pre-mir-146) for 48h. **H-J,** Isolated cardiomyocytes from mice subjected to TAC for 6 weeks were infected with Ad_decoy-146a at (MOI=50) for 48h. The expression of miR-146a (**H**), SUMO1 protein (**I**) and the representative blot (**J**). n=3, *, p<0.05, **, p<0.01 versus the sham control and †, p<0.05, versus failing cardiomyocytes treated with Ad_β-gal, as determined by one-way ANOVA. Data are presented as mean ± s.e.m.

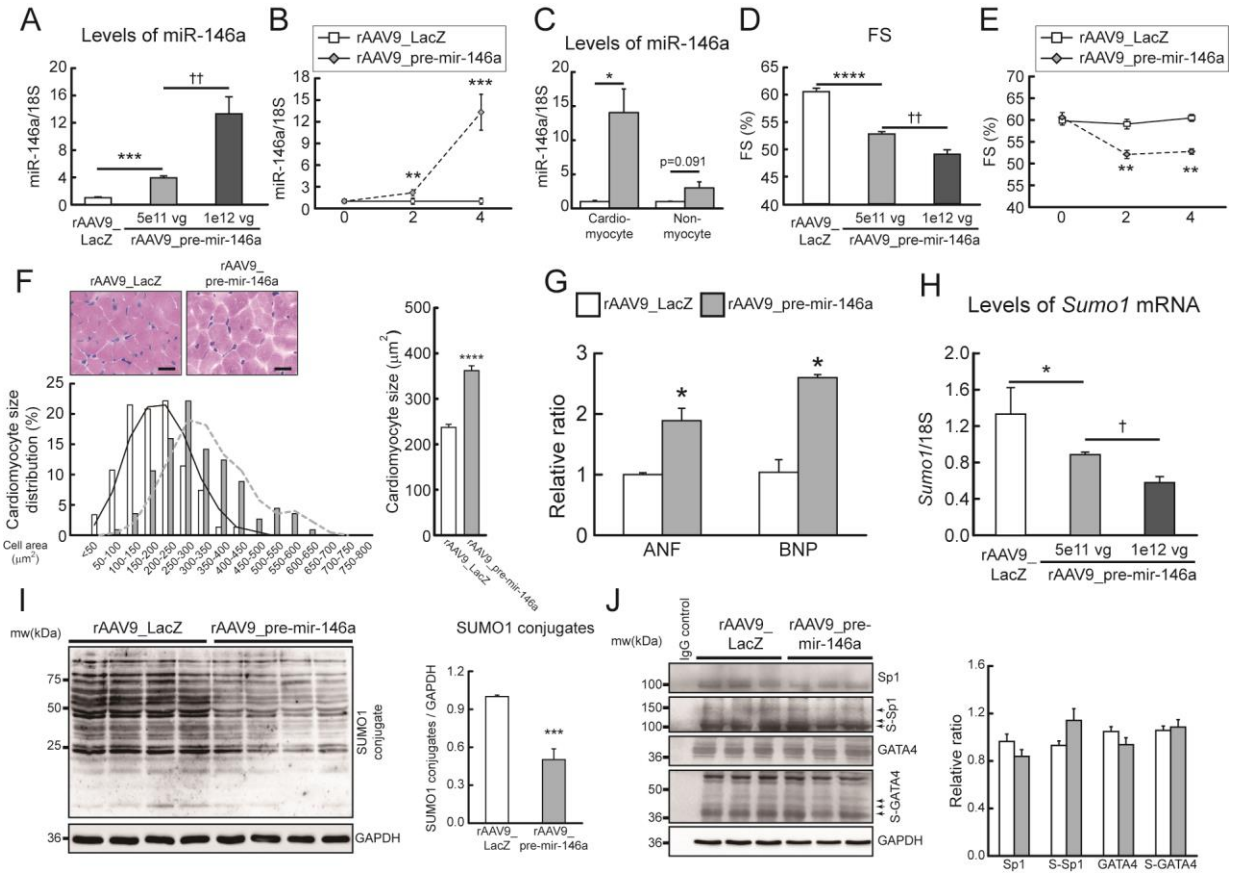

Figure III. Overexpression of miR-146a promotes cardiac dysfunction *in vivo*.

A-C, Levels of miR-146a in a dose-dependent manner (**A**), time-dependent manner (**B**), and isolated fractions of cardiomyocyte or non-myocyte **D** and **E,** Changes in fractional shortening (FS) in a dose-dependent manner (**D**) and time-dependent manner (**E**) (n=6-8). **F,** images of H&E staining **(top, left)**, distribution of cardiomyocyte cross-sectional area (CSA) **(bottom, left)** and mean of CSA **(right)** (n=150~200 cells/4 hearts). Scale bar, 20 μm **G,** mRNA quantification of hypertrophic markers (ANF, BNP). **H,** Levels of SUMO1 in a dose-dependent manner. **I** and **J,** The patterns of global SUMOylation (**I**) and Sp1 or GATA4 SUMOylation (**J**) in wild-type mice received AAV9 carrying pre-mir-146a (rAAV9_pre-mir-146a, 1×10^{12} vg/mouse). *, p<0.05, **, p<0.01, ***, P<0.001 versus mouse infected with rAAV9_LacZ and †, p<0.05, ††, p<0.01 versus mouse infected with rAAV9_pre-mir-146a (5×10^{11} vg.mouse), as determined by one-way ANOVA. Data are presented as mean ± s.e.m. in all panels.

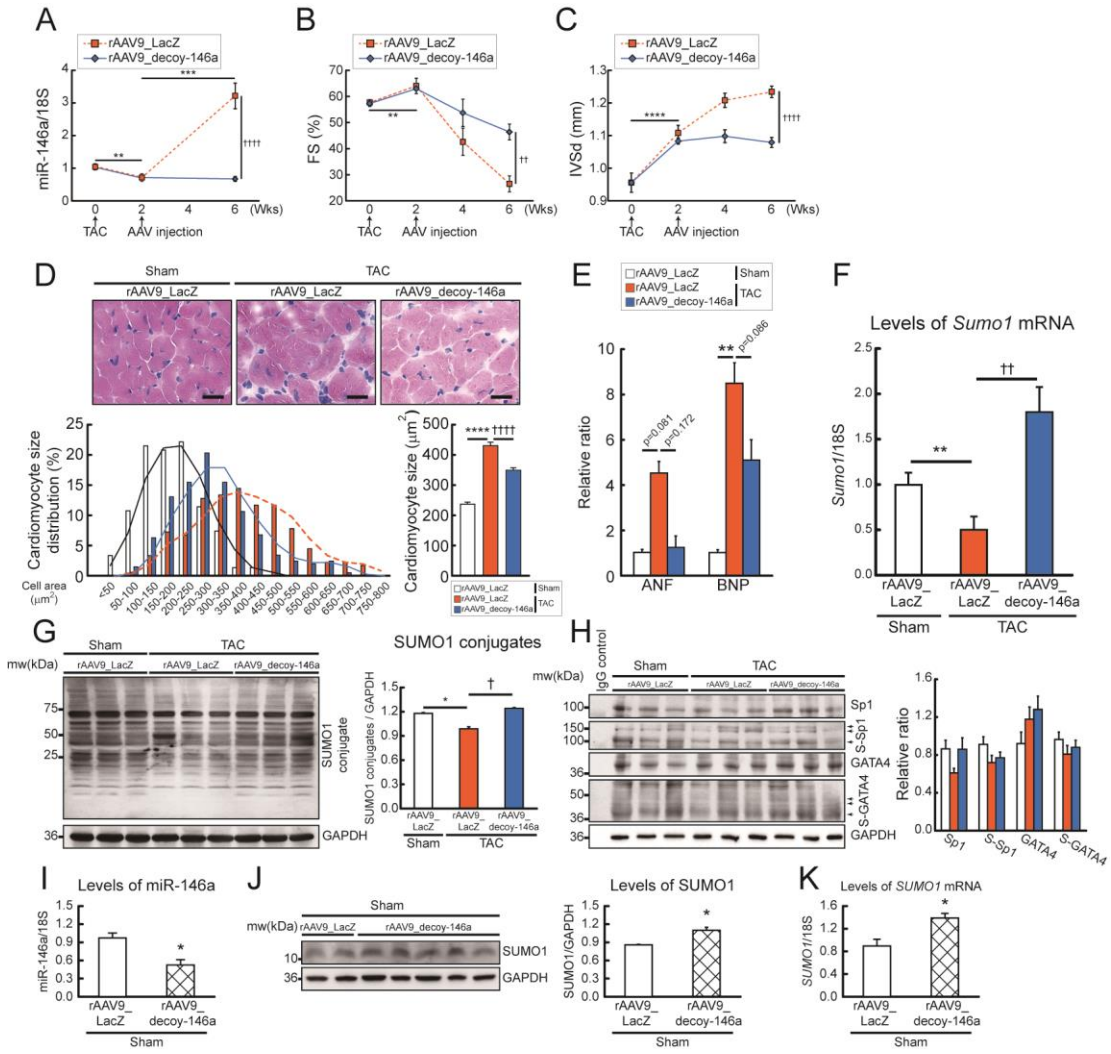

Figure IV. Inhibition of miR-146a prevents cardiac dysfunction under pressure overload *in vivo*.

A, Time-dependent changes in levels of miR-146a (**A**), fractional shortening (FS) (**B**) and wall thickness (interventricular septal end-diastolic dimension, IVSd) (**C**) in TAC-operated mice infected with rAAV9_decoy-146a (5×10^{11} vg/mouse) (n=6-10). **D,** images of H&E staining (**top, left**), distribution of cardiomyocyte cross-sectional area (CSA) (**bottom, left**) and mean of CSA (**right**) (n=150~200 cells/4 hearts). Scale bar, 20 μm **E** and **F,** mRNA quantification of hypertrophic markers (ANF, BNP) (**E**) and SUMO1 (**F**). **G** and **H,** The patterns of global SUMOylation (**G**) and Sp1 or GATA4 SUMOylation (**H**) in TAC-operated mice infected with rAAV9_decoy-146a (5×10^{11} vg/mouse). **I-K**, levels of miR-146a (**I**), SUMO1 protein (**J**) and SUMO1 mRNA (**K**) in wild-type mice received AAV9 carrying decoy-146a (5×10^{11} vg/mouse) (n=5). *, p<0.05, **, p<0.01, ****, p<0.0001 versus the sham mouse and ††, p<0.01,

††††, $p<0.0001$ versus the TAC mouse infected with rAAV9_LacZ, as determined by one-way ANOVA. Data are presented as mean ± s.e.m. in all panels.

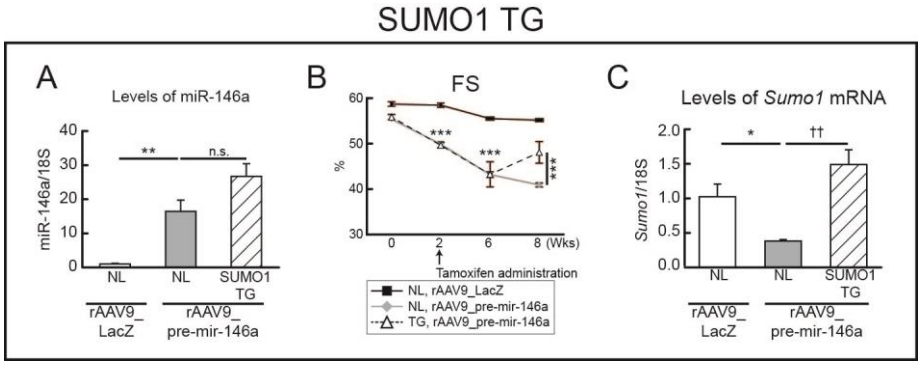

Figure V. Re-expression of SUMO1 attenuates miR-146a-induced cardiac dysfunction *in vivo*.

A and **C,** The levels of miR-146a (**A**) and SUMO1 mRNA (**C**) in SUMO1 TG mice infected with rAAV9_pre-mir-146a (1×10^{12} vg/mouse). **B,** Time-dependent functional effect of SUMO1 re-expression on fractional shortening. n=6-10 *, $p<0.05$, **, $p<0.01$ versus the negative littermate mouse (NL) infected with rAAV9_LacZ and ††, $p<0.01$, ††††, $p<0.0001$ versus the NL mouse infected with rAAV9_pre-mir-146a, as determined by one-way ANOVA. Data are presented as mean ± s.e.m. in all panels.

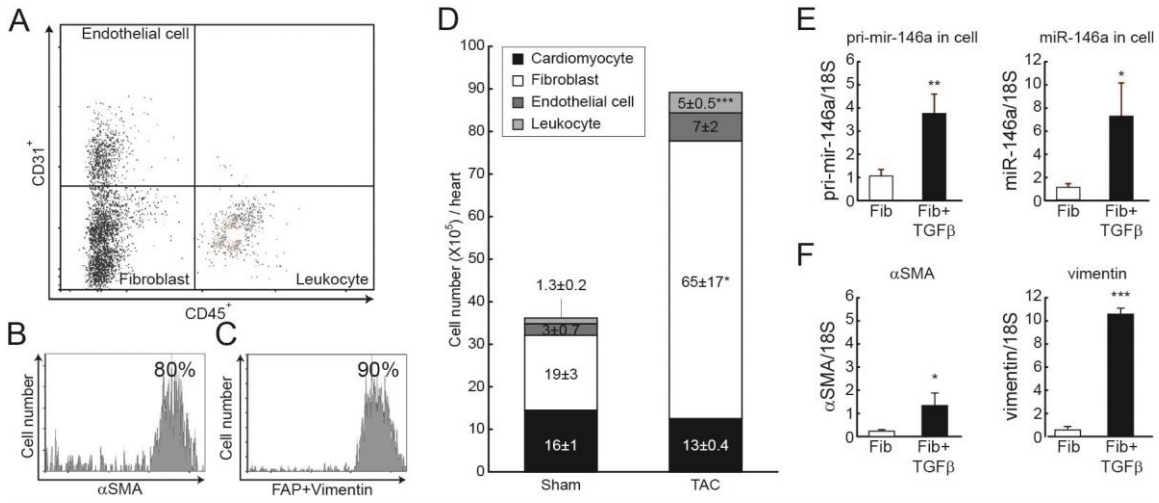

Figure VI. EV-mediated miR-146a transfer reduces cardiomyocyte function.

A-C, Representative FACS analysis of cardiac cell sorting by CD31 and CD45 (**A**). The endothelial cells were defined by the markers $CD31^+$ and $CD45^-$; leukocytes by $CD31^-$ and $CD45^+$; and fibroblasts by $CD31^-$ and $CD45^-$. The purity of the fibroblast fraction was analyzed by flow cytometry using fibroblast-specific markers. Flow cytometric analysis of the α-SMA (**B**), and Fibroblast activation protein (FAP) and Vimentin (**C**) positive cell populations in the fibroblast fraction. **D,** Number of sorted cardiac cells from mouse hearts of sham and TAC-operated mice (TAC, 6 weeks after TAC) (n=5). **E** and **F,** Levels of pri-mir-146a (**E**, **left**), miR-146a (**E**, **right**), αSMA (**F**, **left**) and vimentin (**F**, **right**) in fibroblasts treated with/without TGF-β. *, $p<0.05$, **, $p<0.01$, ***, $p<0.01$ versus the indicated control, as determined by Student's *t*-test. Data are presented as mean ± s.e.m. in all panels.

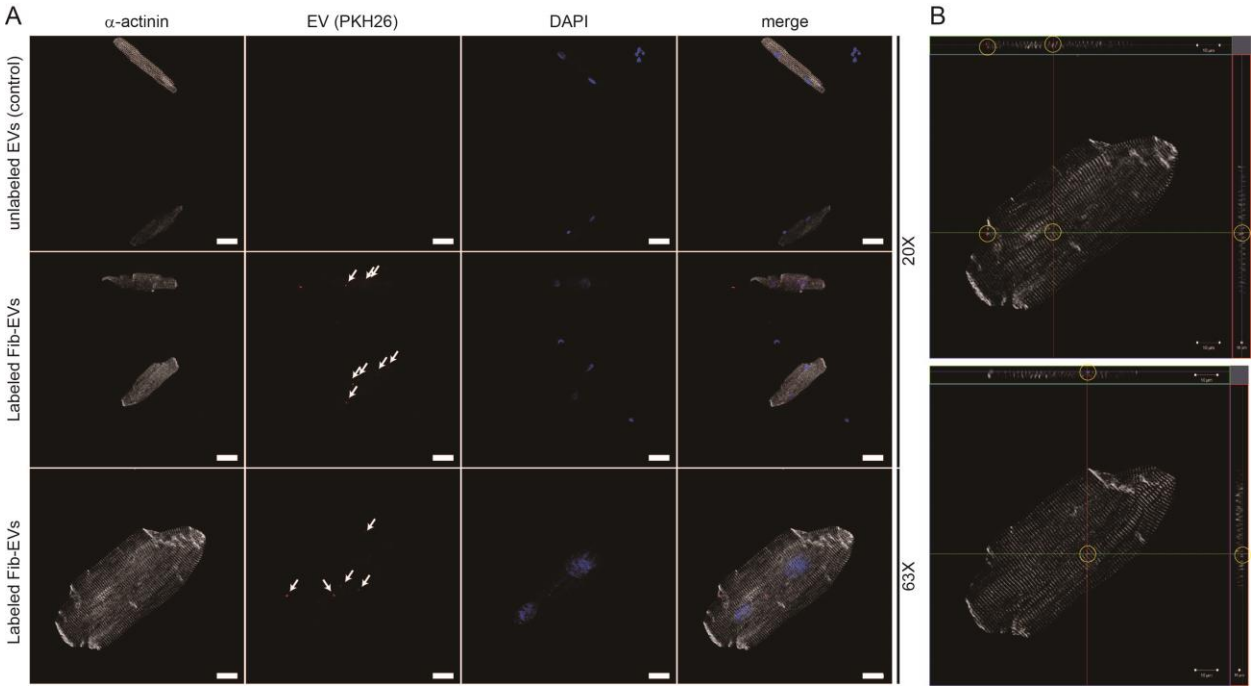

Figure VII. Cardiomyocytes uptake fibroblast-derived EVs (Fib-EVs).

A, Representative images of cardiomyocytes treated with unlabeled EVs (control) or labeled Fib-EVs. Scale bar, 20 μm (top and middle rows) or 10 μm (bottom row). Arrows point to labeled EVs. **B,** Z-axis projection and cross-sectional images (top and right window) of selected cardiomyocytes. Yellow circle: labeled EVs.

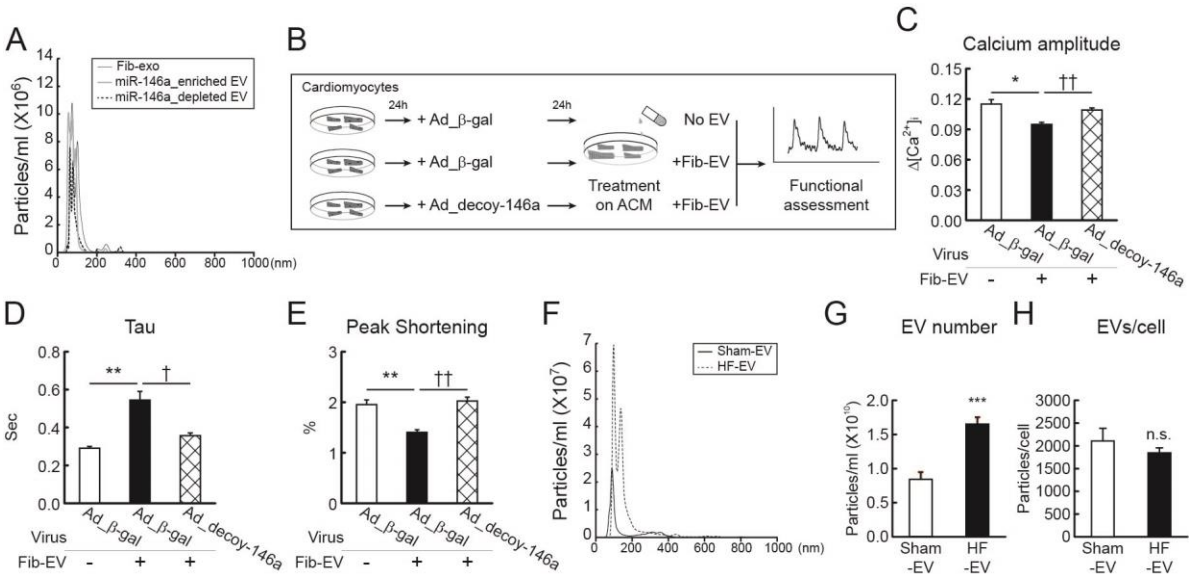

Figure VII. EV-mediated miR-146a transfer reduces cardiomyocyte function.

A, NTA analysis of miR-146a enriched, depleted EVs and fibroblast-derived EVs (Fib-EV). **B**, Scheme depicting a protocol to test protective effects of decoy-146a against Fib-EVs. **C-E,** Averaged data of calcium transient amplitude (**C**), Rate constant for the decay of the Ca^{2+} transient (**D**) and sarcomere length shortening (**E**) (n=3). **F,** NTA analysis of Sham-EV and HF-EV. **G** and **H,** total EV number (**G**) and the number of EVs per single cell (**H**). *, $p<0.05$, **, $p<0.01$, ***, $p<0.01$ versus the indicated control, and †, $p<0.05$, ††, $p<0.01$ versus the cardiomyocytes treated with Fib-EV, as determined by Student's *t*-test. Data are presented as mean ± s.e.m. in all panels.

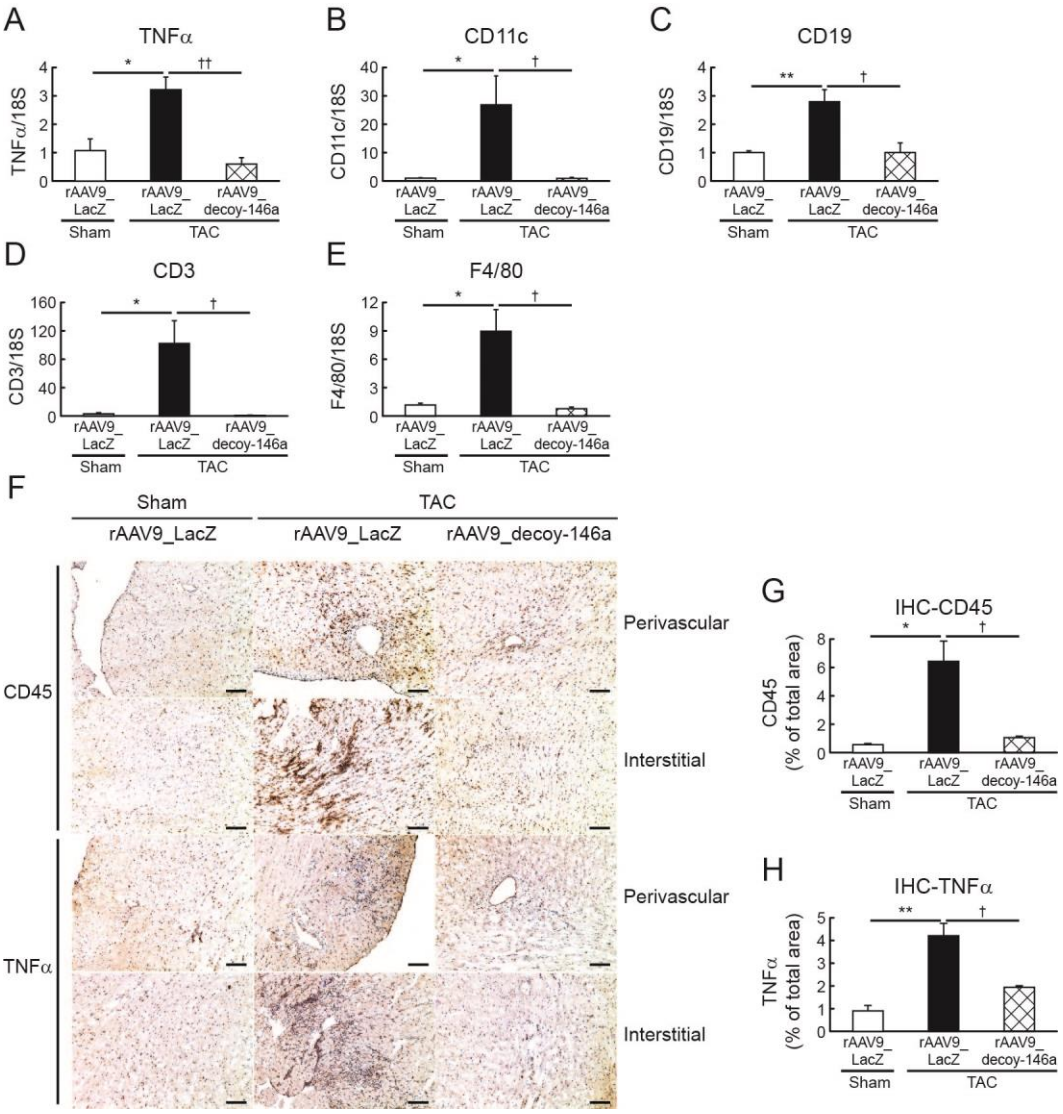

Figure IX. Inhibition of miR-146a does not induce a severe inflammatory response in TAC-induced HF. **A-E,** mRNA quantification of TNF-α (**A**), CD11c (**B**), CD19 (**C**), CD3 (**D**) and F4/80 (**E**) in hearts from sham and TAC mice infected with rAAV9_decoy-146a or rAAV9_LacZ. **F-H,** representative images of immunohistochemistry staining with the pan-inflammatory marker CD45 and TNFα (**F**) and quantifications (**G, H**). Data are presented as mean ± s.e.m. in all panels (n=4). *, p<0.05, **, p<0.01 versus sham mice and †, p<0.05, ††, p<0.01, †††, p<0.001 versus TAC mice infected with rAAV9_LacZ, as determined by Student's *t*-test.

SUPPLEMENTAL TABLES AND SUPPORTING INFORMATION

	Sarcomere length (μm)	Maximal rate of contraction (μm/sec)	Peak shortening (%)	Maximal rate of relaxation (μm/sec)	Baseline Ca^{2+} level (360/380)	Calcium amplitude (Δ360/380)	Tau (sec)
Ad_β-gal	1.8±0.03	-1.1±0.05	3.9±0.2	0.9±0.09	1.6±0.03	0.19±0.01	0.13±0.01
Ad_pre-mir-146a	1.7±0.05	-0.9±0.08*	2.9±0.3*	0.6±0.03*	1.4±0.11	0.13±0.00**	0.18±0.01**

		Sarcomere length (μm)	Maximal rate of contraction (μm/sec)	Peak shortening (%)	Maximal rate of relaxation (μm/sec)	Baseline Ca^{2+} level (360/380)	Calcium amplitude (Δ360/380)	Tau (sec)
Sham	Ad_β-gal	1.8±0.02	-1.8±0.2	6.2±0.5	1.7±0.2	1.5±0.03	0.22±0.01	0.13±0.01
TAC	Ad_β-gal	1.7±0.02	-0.8±0.02**	3.1±0.3**	0.6±0.02**	1.4±0.06	0.06±0.00***	0.19±0.02**
	Ad_decoy-146a	1.7±0.03	-1.3±0.2†	4.9±0.2††	1.3±0.1††	1.3±0.07	0.13±0.02†	0.11±0.02†

Table I. Calcium transient and contractility parameters of cardiomyocytes infected with Ad_pre-mir-146a or Ad_decoy-146a.

Top table, isolated mouse cardiomyocytes were infected with Ad_pre-mir-146a (MOI=50) for 24h. Data represent the mean ± s.e.m. in all panels (n=100-150 cells/4 hearts). *, $p<0.05$, **, $p<0.01$ versus the normal cardiomyocyte treated with Ad_β-gal, as determined by Student's *t*-test.

Bottom table, isolated mouse cardiomyocytes were infected with Ad_decoy-146a (MOI=50) for 24h. Data represent the mean ± s.e.m. in all panels (n=100-150 cells/4 hearts). **, $p<0.01$, ***, $p<0.001$ versus the sham mouse and †, $p<0.05$, ††, $p<0.01$ versus the failing cardiomyocyte treated with Ad_β-gal, as determined by one-way ANOVA.

	rAAV9_ LacZ (Con, n=8)	rAAV9_ pre-mir-146a (Low, n=8)	rAAV9_ pre-mir-146a (High, n=8)
Body weight (g)	35.4±1.0	33.5±0.8	34.3±0.9
Heart weight	133±6	138±5	146±4
HW/BW (mg/g)	3.8±0.1	4.2±0.1	4.3±0.1†
Fractional shortening (%)	60.6±0.6	52.8±0.4**	49.1±0.7†††
Ejection fraction (%)	93.3±0.3	88.0±0.6***	85.8±0.6†††
IVSd (mm)	0.89±0.02	0.93±0.02	0.95±0.01†
IVSs (mm)	1.56±0.06	1.59±0.03	1.53±0.05
LVIDd (mm)	3.39±0.03	3.59±0.08*	3.60±0.03†††
LVIDs (mm)	1.34±0.03	1.73±0.03***	1.81±0.03†††
LVPWd (mm)	0.89±0.01	0.91±0.02	0.92±0.01†
LVPWs (mm)	1.47±0.05	1.49±0.04	1.44±0.03
Heart rate (bpm)	574±7	594±18	566±6

* : rAAV9_LacZ vs rAAV9_pre-mir-146a (Low),
†: rAAV9_LacZ vs rAAV9_pre-mir-146a (High)

Table II. Echocardiographic parameters of mice injected with rAAV9_pre-mir-146a.

Data represent the mean ± s.e.m. of cardiac functional parameters 4 weeks post-injection. HW, heart weight; BW, body weight; HW/BW, ratio of heart weight/body weight; IVSd, interventricular septal end diastole; IVSs, interventricular septal end systole; LVIDd, left ventricular internal dimension-diastole; LVIDs, left ventricular internal dimension-systole; LVPWd, left ventricular posterior wall end diastole; LVPWs, left ventricular posterior wall end systole. *, $p<0.05$, **, $p<0.01$, ***, $p<0.001$ versus the normal mice injected with rAAV9_LacZ and †, $p<0.05$, †††, $p<0.001$ versus the normal mice injected with rAAV9_LacZ, as determined by one-way ANOVA.

	rAAV9_ LacZ (n=6)	rAAV9_ pre-mir-146a (n=6)
Maximum pressure (mmHg)	86±3	77±4
Minimum pressure (mmHg)	4.0±0.4	6.7±0.6
Max dPdt (mmHg/s)	5558±382	3923±215*
Min dPdt (mmHg/s)	-3822±269	-3208±212
Tau (msec)	6.7±0.2	8.5±0.5*
End diastolic volume (μl)	29.8±2.6	43.8±4.4*
End systolic volume (μl)	11.1±2.6	25.7±3.4*
Stroke volume (μl)	29.0±2.4	23.3±1.9
Heart rate (beats/min)	378±63	396±29
Ejection fraction (%)	89.0±3.6	57.5±6.0*

Table III. Hemodynamic parameters of mice injected with rAAV9_pre-mir-146a.

Data represent the mean ± s.e.m. of cardiac functional parameters 4 weeks post-injection. Max dPdt, maximum dP/dt; Min dPdt, minimum dP/dt. *, $p<0.05$, versus the normal mice injected with rAAV9_LacZ, as determined by Student's *t*-test.

	Sham		6 weeks post-TAC	
	rAAV9_ LacZ (sham, n=8)	rAAV9_ decoy-146a (n=5)	rAAV9_ LacZ (TAC, n=9)	rAAV9_ decoy-146a (n=10)
Body weight (g)	34.5±1.2	36.7±1.3	32.8±1.5	32.7±0.9
Heart weight (mg)	123±7	157±2‡	234±10***	203±8†
HW/BW (mg/g)	3.7±0.1	4.3±0.1‡‡	7.2±0.4***	6.2±0.3
Fractional shortening (%)	57.8±0.6	59.7±0.3	26.3±3.1***	44.9±4.2††
Ejection fraction (%)	91.9±0.3	92.9±0.2	56.9±4.8***	79.6±4.5††
IVSd (mm)	0.96±0.03	0.89±0.01	1.23±0.02***	1.08±0.02†††
IVSs (mm)	1.57±0.04	1.49±0.01	1.75±0.05*	1.64±0.07
LVIDd (mm)	3.43±0.02	3.55±0.10	4.22±0.07***	3.83±0.09††
LVIDs (mm)	1.44±0.02	1.40±0.04	3.12±0.17***	2.13±0.20††
LVPWd (mm)	0.98±0.03	1.00±0.04	1.13±0.04*	1.03±0.02†
LVPWs (mm)	1.66±0.07	1.75±0.05	1.84±0.09	1.71±0.06
Heart rate (bpm)	570±7	579±5	557±9	573±8

*: sham vs TAC, †: TAC vs decoy, ‡: sham, rAAV9_LacZ vs sham, rAAV9_decoy-146a

Table IV. Echocardiographic parameters of mice injected with rAAV9_decoy-146a.

Data represent the mean ± s.e.m. of cardiac functional parameters 4 weeks post-injection. HW, Heart weight; BW, Body weight; IVSd, Interventricular septal end diastole; IVSs, Interventricular septal end systole; LVIDd, left ventricular internal dimension-diastole; LVIDs, left ventricular internal dimension-systole; LVPWd, Left ventricular posterior wall end diastole; LVPWs, Left ventricular posterior wall end systole. *, $p<0.05$, **, $p<0.01$, ***, $p<0.001$ versus the sham mouse, †, $p<0.05$, ††, $p<0.01$, †††, $p<0.001$ versus the TAC mouse infected with rAAV9_LacZ and ‡, $p<0.05$, ‡‡, $p<0.01$ versus the sham mouse infected with rAAV9_decoy-146a, as determined by one-way ANOVA.

		TAC	
	rAAV9_ LacZ (sham, n=6)	rAAV9_ LacZ (TAC, n=8)	rAAV9_ decoy-146a (n=7)
Maximum pressure (mmHg)	84±4	101±5*	104±6
Minimum pressure (mmHg)	5.6±0.9	6.3±0.6	4.7±0.3†
Max dPdt (mmHg/s)	5952±1032	3491±128*	4900±319††
Min dPdt (mmHg/s)	-3671±355	-2493±210**	-3750±321††
Tau (msec)	8.2±0.8	12.2±1.0**	8.1±0.3††
End diastolic volume (μl)	26±1	76±7***	48±4††
End systolic volume (μl)	10±1.7	44±7***	21±5†
Stroke volume (μl)	26±2	32±3	37±5
Heart rate (beats/min)	368±12	336±15	360±28
Ejection fraction (%)	80±5	49±4**	73±6†

*: sham vs TAC, †: TAC vs decoy

Table V. Hemodynamic parameters of mice injected with rAAV9_decoy-146a.

Data represent the mean ± s.e.m. of cardiac functional parameters 4 weeks post-injection. Max dPdt, maximum dP/dt; Min dPdt, minimum dP/dt. *, $p<0.05$, **, $p<0.01$, ***, $p<0.001$ versus the sham mouse and †, $p<0.05$, ††, $p<0.01$, versus the TAC mouse infected with rAAV9_LacZ, as determined by one-way ANOVA.

	rAAV9_LacZ	rAAV9_pre-mir-146a	
	NL (n=8)	NL (n=8)	TG (n=5)
Body weight (g)	30.5±1.3	30.7±0.7	29.6±0.5
Heart weight (mg)	133±6	152±8	163±22
HW/BW (mg/g)	3.8±0.1	4.9±0.2***	5.5±0.8
Fractional shortening (%)	59.2±0.9	40.9±0.4***	48.1±2.4††
Ejection fraction (%)	92.6±0.5	78.2±0.5***	84.7±2.0††
IVSd (mm)	0.87±0.03	0.91±0.02	0.90±0.02
IVSs (mm)	1.52±0.07	1.37±0.03	1.35±0.03
LVIDd (mm)	3.28±0.05	3.55±0.07**	3.20±0.09††
LVIDs (mm)	1.34±0.01	2.03±0.05***	1.67±0.12††
LVPWd (mm)	0.85±0.01	0.90±0.01*	0.86±0.02
LVPWs (mm)	1.44±0.05	1.26±0.02**	1.29±0.04
Heart rate (bpm)	591±13	579±3	572±9

*: NL, rAAV9_LacZ vs NL, rAAV9_pre-mir-146a,
†: NL, rAAV9_pre-mir-146a vs TG, rAAV9_pre-mir-146a

Table VI. Echocardiographic parameters of SUMO1 TG mice injected with rAAV9_pre-mir-146a.

Data represent the mean ± s.e.m. of cardiac functional parameters 8 weeks post-injection. NL, Negative littermate; SUMO1 TG, Cardiac-specific Cre/loxP-conditional *Sumo1*-transgenic mice; HW, Heart weight; BW, Body weight; IVSd, Interventricular septal end diastole; IVSs, Interventricular septal end systole; LVIDd, left ventricular internal dimension-diastole; LVIDs, left ventricular internal dimension-systole; LVPWd, Left ventricular posterior wall end diastole; LVPWs, Left ventricular posterior wall end systole. *, $p<0.05$, **, $p<0.01$, ***, $p<0.001$ versus the NL mouse infected with rAAV9_LacZ and †, $p<0.05$, ††, $p<0.01$, †††, $p<0.001$ versus the NL mouse infected with rAAV9_pre-mir-146a, as determined by one-way ANOVA.

	Cardiomyocyte	Fibroblast	Leukocyte	Endothelial cell	Total cell
Sham	1.6E+06 ± 1.4E+05	1.9E+06 ± 3.0E+05	1.3E+05 ± 1.8E+04	3.0E+05 ± 7.0E+04	4.0E+06 ± 4.6E+05
TAC	1.3E+06 ± 0.4E+05***	6.5E+06 ± 1.7E+05*	4.8E+05 ± 5.0E+05***	6.6E+05 ± 2.0E+05	9.0E+06 ± 1.8E+05*
	% Cardiomyocyte	% Fibroblast	% Leukocyte	% Endothelial cell	
Sham	41 ± 4	48 ± 4	4 ± 1	7 ± 1	
TAC	16 ± 3**	71 ± 5**	6 ± 1*	8 ± 2	

Table VII. Cardiac cellular composition.

Isolated cardiac cells were sorted with FACS and analyzed. Data represent the mean ± s.e.m. (n=5). *, $p<0.05$, **, $p<0.01$, ***, $p<0.001$ versus the sham mouse, as determined by one-way ANOVA.

	Sarcomere length (μm)	Maximal rate of contraction (μm/sec)	Peak shortening (%)	Maximal rate of relaxation (μm/sec)	Baseline Ca^{2+} level (360/380)	Calcium amplitude (Δ360/380)	Tau (sec)
no treatment (control)	1.7 ± 0.02	-1.1 ± 0.04	4.1 ± 0.1	1.0 ± 0.1	1.5 ± 0.04	0.197 ± 0.014	0.127 ± 0.006
Fib-EV	1.7 ± 0.02	-0.7 ± 0.2*	2.3 ± 0.1***	0.5 ± 0.04**	1.4 ± 0.05	0.131 ± 0.004*	0.217 ± 0.017**

	Sarcomere length (μm)	Maximal rate of contraction (μm/sec)	Peak shortening (%)	Maximal rate of relaxation (μm/sec)	Baseline Ca^{2+} level (360/380)	Calcium amplitude (Δ360/380)	Tau (sec)
Fib-EV	1.7 ± 0.02	-0.7 ± 0.2	2.3 ± 0.1	0.5 ± 0.04	1.4 ± 0.05	0.131 ± 0.004	0.217 ± 0.017
miR-146a-enriched EV	1.8 ± 0.03	-0.4 ± 0.02*	1.5 ± 0.2*	0.4 ± 0.01*	1.5 ± 0.03	0.108 ± 0.006*	0.296 ± 0.020*
miR-146a-depleted EV	1.7 ± 0.02	-0.9 ± 0.06	3.0 ± 0.2†	0.7 ± 0.04†	1.5 ± 0.07	0.158 ± 0.004††	0.160 ± 0.012†

	Sarcomere length (μm)	Maximal rate of contraction (μm/sec)	Peak shortening (%)	Maximal rate of relaxation (μm/sec)	Baseline Ca^{2+} level (360/380)	Calcium amplitude (Δ360/380)	Tau (sec)
Sham-EV	1.7±0.01	-1.2±0.07	4.5±0.3	1.1±0.07	1.5±0.02	0.16±0.01	0.124±0.005
HF-EV	1.7±0.01	-0.7±0.04**	2.4±0.1**	0.7±0.08*	1.5±0.04	0.12±0.01*	0.146±0.004**

Table VIII. Calcium transient and contractility parameters of cardiomyocytes treated with EVs derived from fibroblasts or whole mouse hearts.

Top table, isolated mouse cardiomyocytes were treated with fibroblast-derived EVs at 2000 particles/cell for 24h and analyzed. Data represent the mean ± s.e.m. (n=60-80 cells/3 hearts). *, $p<0.05$, **, $p<0.01$, ***, $p<0.001$ versus the non-treated group, as determined by Student's *t*-test.

Middle table, isolated mouse cardiomyocytes were treated with indicated EVs at 2000 particles/cell for 24h and analyzed. Data represent the mean ± s.e.m. (n=60-80 cells/3 hearts). *, $p<0.05$ versus the fibroblast-derived EVs-treated group and †, $p<0.05$, ††, $p<0.01$ versus the fibroblast-derived EVs-treated group, as determined by one-way ANOVA.

Bottom table, isolated mouse cardiomyocytes were treated with EVs from failing heart at 2000 particles/cell for 24h and analyzed. Data represent the mean ± s.e.m. (n=60-80 cells/3 hearts). *, $p<0.05$, **, $p<0.01$ versus the control cardiomyocytes treated with EVs from the sham heart, as determined by Student's *t*-test.

	Sham	2 weeks post-TAC (before injection)	
	rAAV9_ LacZ (Sham, n=8)	rAAV9_ LacZ (TAC, n=9)	rAAV9_ decoy-146a (n=10)
Body weight (g)	31.1±0.7	31.7±1.1	30.3±0.6
Heart weight (mg)	N.A.	N.A.	N.A.
HW/BW (mg/g)	N.A.	N.A.	N.A.
Fractional shortening (%)	58.1±0.5	63.6±1.4**	62.9±1.2††
Ejection fraction (%)	92.1±0.3	94.6±0.6**	94.5±0.5††
IVSd (mm)	0.88±0.03	1.09±0.01***	1.08±0.01†††
IVSs (mm)	1.63±0.07	1.74±0.04	1.75±0.02
LVIDd (mm)	3.43±0.04	3.22±0.06*	3.22±0.04††
LVIDs (mm)	1.43±0.02	1.16±0.07**	1.20±0.05††
LVPWd (mm)	0.86±0.01	1.04±0.03***	1.06±0.02†††
LVPWs (mm)	1.53±0.05	1.81±0.06**	1.74±0.04††
Heart rate (bpm)	567±17	555±4	566±5

*: sham vs TAC+rAAV9_LacZ, †: sham vs rAAV9_decoy-146a

Table IX. Echocardiographic parameters of mice subjected to TAC surgery before the gene transfer.

Data represent the mean ± s.e.m. of cardiac functional parameters 4 weeks post-injection. HW, Heart weight; BW, Body weight; IVSd, Interventricular septal end diastole; IVSs, Interventricular septal end systole; LVIDd, left ventricular internal dimension-diastole; LVIDs, left ventricular internal dimension-systole; LVPWd, Left ventricular posterior wall end diastole; LVPWs, Left ventricular posterior wall end systole. *, $p<0.05$, **, $p<0.01$, ***, $p<0.001$ versus the sham mouse, †, $p<0.05$, ††, $p<0.01$, †††, $p<0.001$ versus the TAC mouse infected with rAAV9_LacZ, as determined by one-way ANOVA.

SUPPEMENTAL REFERENCES

1. Oh JG, Jeong D, Cha H, Kim JM, Lifirsu E, Kim J, Yang DK, Park CS, Kho C, Park S, Yoo YJ, Kim DH, Hajjar RJ, Park WJ. PICOT increases cardiac contractility by inhibiting PKCzeta activity. *J Mol Cell Cardiol.* 2012;53(1):53-63.

2. Oh JG, Kim J, Jang SP, Nguen M, Yang DK, Jeong D, Park ZY, Park SG, Hajjar RJ, Park WJ. Decoy peptides targeted to protein phosphatase 1 inhibit dephosphorylation of phospholamban in cardiomyocytes. *J Mol Cell Cardiol.* 2012;56:63-71.

3. Kho C, Lee A, Jeong D, Oh JG, Chaanine AH, Kizana E, Park WJ, Hajjar RJ. SUMO1-dependent modulation of SERCA2a in heart failure. *Nature.* 2011;477(7366):601-605.